Natural Hazards
https://doi.org/10.1007/s11069-024-06637-7

ORIGINAL PAPER

Reconnaissance survey and macroseismic intensity estimation of the 26th May 2021 Gisenyi (Rwanda) earthquake (M_w 5.1) as a contribution to the seismic hazard assessment in a volcano-tectonic environment

Francois Hategekimana[1,2] · Young-Seog Kim[1] · Himanshu Mittal[3] · Fils Vainqueur Byiringiro[2] · Mohammed S. M. Adam[1] · Digne Edmond Rwabuhungu Rwatangabo[2] · Sambit Prasanajit Naik[1,4]

Received: 7 January 2024 / Accepted: 18 April 2024

Abstract
On 26th May 2021, an earthquake with a moment magnitude M_w 5.1 hit the densely populated cities of Gisenyi (Rwanda) and Goma (D.R. Congo) which sit on the active East African Rift System. It was one of the largest earthquakes associated with the 2021 Mount Nyiragongo eruption. Although of moderate magnitude, the earthquake substantially damaged manmade structures. This paper presents field observations on the geotechnical impact, building damage, and factors contributing to the heightened destruction caused by this moderate earthquake. The damage pattern observed in the field indicates that masonry structures with inadequate seismic detailing were the most damaged buildings. In addition, the statistical analysis of the damaged buildings indicates most of the damaged structures were located in plains covered by volcanic soil. The intensity of the waves was estimated using the building damage data based on the European Macroseismic Scale (EMS-98). An intensity distribution map was generated for the surveyed area, suggesting EMS-98 intensity of VIII or IX along the eastern basin boundary fault and VII around the cities of Goma and Gisenyi where the land is composed of black cotton soil of volcanic origin. The higher intensity values along the eastern basin-bounding fault indicate that a reevaluation of the seismic hazard for the region is necessary. Since this is the first-ever such damage survey for the region, the developed intensity map can be used to understand the correlation between the intensity of the ground motion and damage severity which contributed to the seismic hazard assessment of the study area.

Keywords East African Rift System · Gisenyi (Rwanda) · Goma (D.R. Congo) · EMS-98 · Seismic hazard

Extended author information available on the last page of the article

Published online: 08 May 2024

1 Introduction

On 26 May 2021, a M_w 5.1 hit the densely populated cities of Gisenyi and Goma. It was one of the highest magnitude earthquakes to hit the area since the 18th century. As reported by the Rwanda National Seismic Network, operated by the Rwanda Mines, Petroleum and Gas Board (RMB), the earthquake occurred at 05:46 am, Kigali time. Several aftershocks were recorded after the Gisenyi earthquake which were concentrated along the eastern boundary of the Kivu rift. The rift is bounded by eastern and western basin-bounding normal faults associated with the rift system (Fig. 1a-b). The Gisenyi earthquake occurred after the Nyiragongo volcanic eruption on 22nd May 2021 (Boudoire et al. 2022). According to the government of Rwanda, this Gisenyi earthquake caused widespread damage in the DR Congo and Rwanda. Around, 1,500 houses were destroyed by the earthquake in the Rubavu District.

Macroseismic intensity refers to the classification of the severity of ground shaking based on the observed effects during an earthquake (Dengler and McPherson 1993; Serva 1994; Esposito et al. 1997; Grünthal et al. 1998; Michetti et al. 2004; Cua et al. 2010). Macroseismic intensity has been used as an index to describe the effects of damaging earthquakes (Allen et al. 2009; Silva and Horspool 2019; Weixiao et al. 2021; Naik et al. 2020; Naik et al. 2023). Moreover, it has been applied in volcano-tectonic environments like Mt. Etna, Italy to assess surface faulting (Azzaro et al. 1998, 1999, 2000; Ferreli et al. 2002; Tringali et al. 2023). Additionally, it has been utilized for seismic zonation in Ischia Island, Italy (Vassallo et al. 2021). This approach is more suitable for seismic hazard management, with

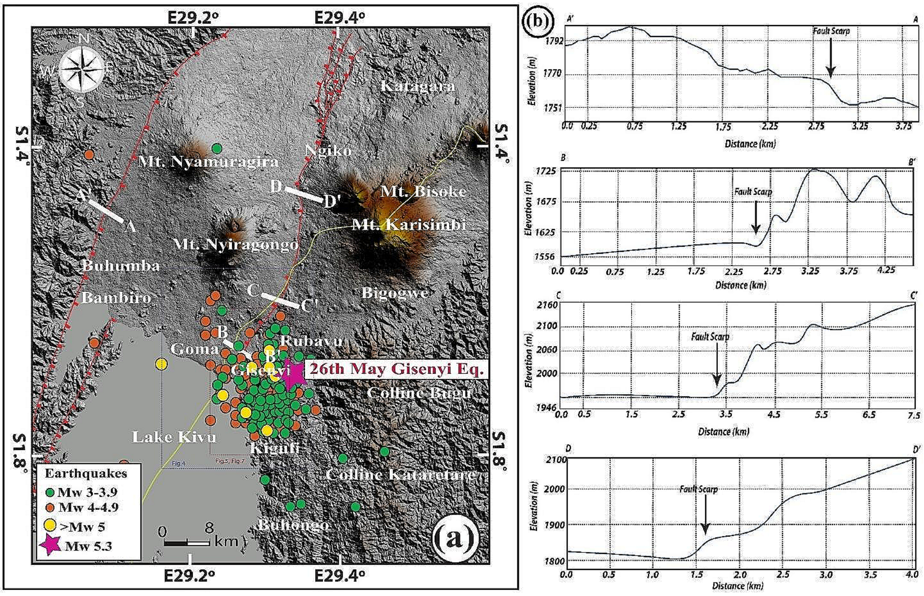

Fig. 1 **a** ALOS DEM map showing the distribution of earthquakes associated with the Nyiragongo volcanic eruption on 22 May 2021 and the major structural features around the study area (12.5 m ALOS DEM data were taken from https://search.earthdata.nasa.gov/search), **b** Elevation profiles across the major faults around the study area. The white solid line indicates the location of the elevation profile shown in Fig. 1b. The blue-dotted box marks the location of Fig. 4, and the red-dotted box denotes the location of Figs. 5 and 7

little or no strong motion data. Since macroseismic intensity reflects the degree of damage induced by an earthquake, it is used for rapid loss modeling, post-disaster reconnaissance surveys, and relief support for the affected regions (Grünthal 1998; Porfido et al. 2007; Earle et al. 2009; Kamer et al. 2009; Musson et al. 2010; Trendafiloski et al. 2011; C.S.LL. PP. 2018; Michelini et al. 2019; Gomez-Capera et al. 2020; Naik et al. 2024). Despite the widespread acceptance of the use of site-specific ground motion intensity measures (IMs) to characterize earthquakes in the case of ground response analysis and design of lifeline structures (C.S.LL.PP. 2018), macroseismic intensity is still widely used in those areas where the seismic monitoring network is sparse or even absent. The macroseismic intensity and resulting ShakeMap derived from it can be used for a rapid loss assessment and a vulnerability analysis of existing structures in an area of interest (Wald et al. 1999; Giovinazzi and Lagomarsino 2004; Michelini et al. 2019). Additionally, macroseismic intensity can be used to determine the earthquake parameters such as event magnitude, peak ground accelerations, (PGA), peak ground velocity (PGV), and peak ground displacements (PGD) based on their empirical relationships (Sibol et al. 1987; Giovinazzi and Lagomarsino 2004; Faenza and Michelini 2010; Azzaro et al. 2011; Nappi et al. 2018; Zanini et al. 2019; Gomez-Capera et al. 2020; Naik et al. 2023b, 2024).

Several intensity scales are utilized to qualitatively evaluate the impact and effects of earthquakes on individuals, the built environment, and natural landscapes. These include the Modified Mercalli Intensity (MMI) scale, the Japan Meteorological Agency (JMA) Seismic Intensity Scale, the China Seismic Intensity Scale (CSIS), the Environmental Seismic Intensity (ESI 2007) scale for assessing primary and secondary environmental effects (Michetti et al. 2007), and the European Macroseismic Scale (EMS-98) (Wood and Neumann 1931; Grünthal, 1998; Supino et al. 2019; Naik et al. 2023a, b). Among these, the EMS-98 scale has recently gained widespread international adoption (Silveira et al. 2003; Galea 2007; Tertulliani et al. 2018; Buforn and Udías 2022; Sarabia Gómez et al. 2022; Martin et al. 2022; Triantafyllou et al. 2022; Tertulliani and Graziani 2022; Del Mese et al. 2023) due to its potential for upgrades and the inclusion of new building types, particularly those designed to be earthquake-resistant, which were not considered during the development of other traditional scales (Del Mese et al. 2023). The EMS-98 scale was designed not only with seismologists in mind but also civil engineers and other potential users (Del Mese et al. 2023). For our current study, we applied the EMS-98 intensity scale to the most damaging earthquake in recent Rwandan history, considering the types of buildings that closely match the macroseismic criteria described in the EMS-98 scale. Although the earthquake did not have a high magnitude, it produced considerable damage as a result of having a very shallow hypocenter. This region is highly populated and is located along the western flank of the East African Rift System, which is a seismically active branch of the African Rift System. Therefore, we systematically surveyed the building damage pattern to understand the macroseismic intensity distribution as well as other seismic parameters, that contributed to the assessment of seismic hazard.

In this study, we have constructed a macroseismic intensity map based on the damage survey collected in the field and on information derived from standard questionnaires in the macroseismic field survey. We have assigned EMS-98 values for 300 locations, according to the classic definitions, in part to facilitate comparisons between the present earthquake damage pattern observations in the field and those determined for other earthquakes. The intensity pattern observed for the 2021 Gisenyi earthquake highlights the importance of heterogeneous building types and variations of local geology for resultant structural damage.

2 Seismotectonic setting of the area

Seismicity in the East African Rift System (EARS) is mainly controlled by two factors: (1) extension associated with continental rifting, and (2) volcanism. Previous studies (Yang and Chen 2010) revealed that the western branch of the EARS is more seismically active, while the eastern branch is more volcanically active (Fig. 2a). Gisenyi, northwestern Rwanda, lies along the Kivu Rift, which is part of the western branch of the East African Rift System (Fig. 2a-b). The Kivu rift is an extensional area with an extension rate of ~ 2.3–2.8 mm/yr (Stamps et al. 2008; Saria et al. 2014; Geirsson et al. 2017).

The Kivu Rift has been recognized as seismically active since the first half of the 20th century (Cornet 1910; Passau 1911, 1912; Krenkel 1922; Sieberg 1932; Figs. 1 and 2). Earthquakes above magnitude 5 are rare in the Kivu basin (Barth et al. 2007; Mavonga 2007; Mavonga and Durrheim 2009; Delvaux and Barth 2010). According to the USGS catalog (1973-present) (Fig. 2b), the 2021 Mw 5.3 Gisenyi earthquake was one of the largest earthquakes in the region in addition to the 2002 Mw 6.2 Kalehe earthquake (Wauthier et al. 2015), the Mw 5.9 Bukavu earthquake (d'Oreye et al. 2011) and the 2015 M_w 5.8 Lwiro earthquake (Geirsson et al. 2017) which was followed by a 5.5 Mw aftershock. The 2015 Mw 5.8 Lwiro earthquake led to the death of 3 people with many injured. Seismic activity in the Kivu Rift is closely related to volcanic activity. In addition to larger earthquakes, moderate earthquakes were also recorded in 1977 and 2002, which coincided with the only two recorded fissure eruptions of the Nyiragongo volcano. The activities of Nyiragongo and Nyamulagira are probably directly related to the opening of the Western Rift Valley (Kasahara et al. 1991; Wauthier et al. 2015). The 2002 eruption of the Nyiragongo volcano,

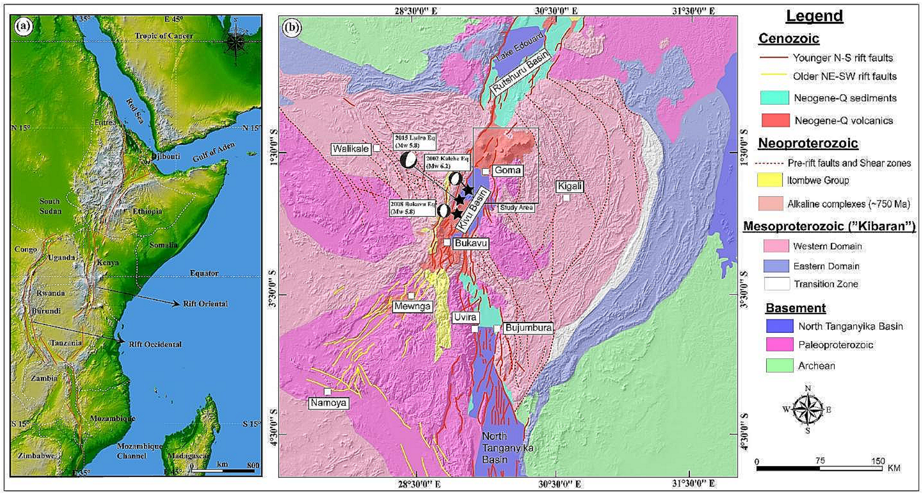

Fig. 2 Map showing **a** the distribution of major faults along the East African Rift System (EARS), **b** simplified geological map of the western part of the EARS focusing on Rwanda and DR Congo (modified after Delvaux et al. 2017)

for example, was associated with regional rifting events (Komorowski et al. 2002/2003; Tedesco et al. 2007a, b). This devastating eruption left more than 120, 000 people homeless (Tedesco et al. 2007a). Moreover, the 1977 eruption of the Nyiragongo volcano occurred four days after a Mw 5.3 event struck the Bukavu area (Hamaguchi et al. 1992). It should be noted that small to moderate earthquakes occur frequently in this region, and many of them are not related to eruptions. This applies both to the Bukavu earthquake itself and to the two M > 4 earthquakes that occurred in October 2008 approximately 50 km north of Goma, DRC (d'Oreye et al. 2011).

3 Methodology of macroseismic survey

Earlier macroseismic intensity scales, such as Medvedev–Sponheuer–Karnik (MSK), and Mercalli-Cancani-Sieberg (MCS), are often ambiguous in defining structural damage levels, grades and vulnerabilities (Musson et al. 2010; Grünthal et al. 1998; Li et al. 2020; Cito et al. 2022; Del Mese et al. 2023). The implementation of the EMS-98 was an important step that substantially raised the quality of traditional intensity assignments (Cito et al. 2022). The EMS-98 has 12 divisions, and each division describes distinct observations or damage patterns due to the earthquake intensity (Table 1). For assigning intensity values higher than V, as per the EMS-98 scale, detailed field reconnaissance observations gathered using strict data collection protocols are required (Contreras et al. 2021). The EMS-98 intensity values help in the characterization of the seismic vulnerability of each building and places them in a vulnerability class range from A–F, where A indicates the most vulnerable structures and F the least. Using the EMS-98 intensity scale, detailed post-earthquake observations can help to assign an intensity level at a particular location considering the percentage of buildings damaged at that location (Grünthal, 1998, Spence and Foulser-Piggott 2014; Abrahamczyk et al. 2017; Cito et al. 2022). It is noted that Rwanda and Congo do not have any specific building codes. The study area possesses heterogeneous building types (Fig. 3) with some buildings made of mud, bricks, or stones without any formal engineering approach. Some buildings are engineered with pillars and beams (Fig. 3). For our current study, we have applied the EMS-98 intensity scale, taking into account the types of buildings that closely match the macroseismic criteria described in the EMS-98 scale (Table 1) which are presented in the subsequent sections.

3.1 Macroseismic survey

In this study, we have conducted a detailed field reconnaissance survey around the Rugerero, Gisenyi, and Rubavu Sectors of the Rubavu District, Rwanda, which were highly affected by the earthquake (Fig. 2). The epicentral region of the 26th May 2021 earthquake in Rwanda and DR Congo has no standard criteria for assessing the macroseismic intensity. This is the very first time an attempt has been made to conduct a detailed post-earthquake survey to assess the macroseismic intensity as well as other ground motion parameters leading to the preparation of a seismic intensity map around the Gisenyi and Rubavu sectors of Rwanda. We have examined the effects of the earthquake on the natural and built environments. Due to international border issues, we were unable to conduct a detailed damage survey in the affected areas of DR Congo.

Table 1 Damage description as per the EMS-98 intensity scale

Definition	Description of Observed Effects	EMS-98
Not felt	Not felt.	I
Scarcely felt	Felt only by very few individual people at rest in houses.	II
Weak Felt	Felt Indoors by a few people. People at rest feel a swaying or light trembling.	III
Largely observed	Felt indoors by many people, and outdoors by very few. A few people are awakened. Windows, doors and dishes rattle.	IV
Strong	Felt indoors by most, outdoors by few. Many sleeping people awake. A few are frightened. Buildings tremble throughout. Hanging objects swing considerably. Small objects are shifted. Doors and windows swing open or shut.	V
Slightly damaging	Many people are frightened and run outdoors. Some objects fall. Many houses suffer slight non-structural damage like hairline cracks and fall of small pieces of plaster.	VI
Damaging	Most people are frightened and run outdoors. Furniture is shifted and objects fall from shelves in large numbers. Many well-built ordinary buildings suffer moderate damage: small cracks in walls, fall of plaster, and parts of chimneys fall down; older buildings may show large cracks in walls and failure of fill-in walls.	VII
Heavily damaging	Many people find it difficult to stand. Many houses have large cracks in the walls. A few well-built ordinary buildings show serious failure of walls, while weak older structures may collapse.	VIII
Destructive	General panic. Many weak constructions collapse. Even well-built ordinary buildings show very heavy damage: serious failure of walls and partial structural failure.	IX
Very destructive	Many ordinary well-built buildings collapse.	X
Devastating	Most ordinary well-built buildings collapse, even some with good Earthquake-resistant designs are destroyed.	XI
Completely devastating	Almost all buildings are destroyed	XII

3.1.1 Effect on natural environment

The 2021 Gisenyi earthquake, which was associated with the Mount Nyiragongo eruption, caused several secondary ground effects, including gas emission and the formation of ground cracks. Boudoire et al. (2022) reported numerous ground cracks, which were primarily concentrated around Goma and Gisenyi, may be related to the magmatic processes associated with the 2021 Mount Nyiragongo eruption (Fig. 4). During our post-earthquake field survey, we also mapped several ground cracks, predominantly located along the eastern basin-bounding faults of the Kivu Rift. Most of these ground cracks exhibit vertical displacements of 3–5 cm (Fig. 4b-d) with an N-S/NNE-SSW orientation which may be associated with the movement of the eastern basin boundary fault during the 26th May 2021 earthquake. Due to their limited number, we did not utilize the ground cracks for our macroseismic intensity estimation in this study.

3.1.2 Effects of the 2021 Gisenyi earthquake on built environment

In Gisenyi City, in the western part of Rwanda, the macroseismic data collected to estimate the seismic intensity utilized the traditional methods of field surveys as well as the distribution of questionnaires immediately after the 2021 Gisenyi earthquake (Supplementary

Fig. 3 Main building types found in the Gisenyi and Rubavu areas

Information S1). The evaluation was based on assessing how ground motion affected people, household items, and caused damage to buildings in Gisenyi City. The macroseismic investigation was carried out through field survey questionnaires where the participants were asked to describe personally observed effects. Twenty-three questions were prepared and distributed to residents of the Gisenyi and Rubavu sectors (Supplementary Information S1). Those questions covered three main topics including people's perception of the strength of the quake, effects on objects (fixed and moveable), and effects on infrastructures.

To determine the macroseismic intensity (Table 1) around the epicentral area, it was mandatory to identify the types of buildings and the effect the earthquakes on them. Considering the responses to the questionnaires and field survey the heterogeneous building types were identified (Fig. 3). They are divided into five categories: (1) Traditional mud huts, (2) mud houses without any brick elements, (3) brick houses with mud reinforcement, (4) brick houses with cement reinforcement, and (5) modern single or multistory brick houses with or

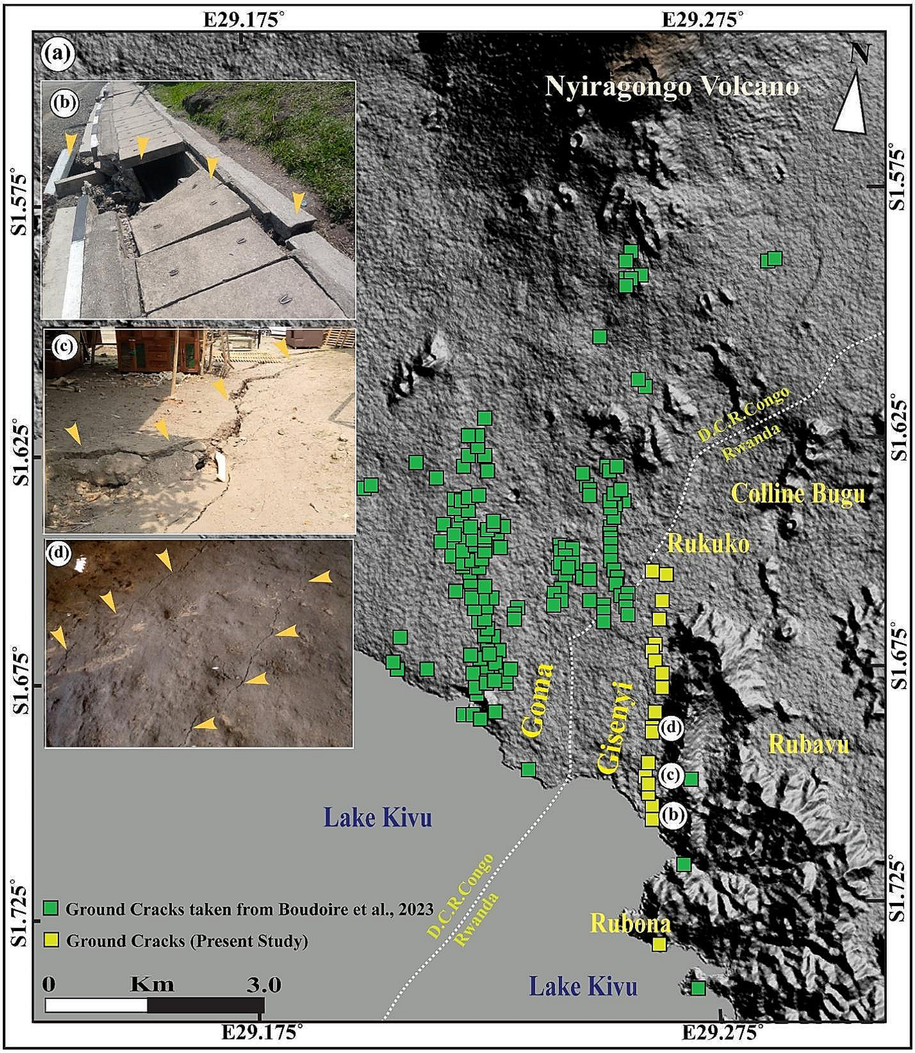

Fig. 4 Ground cracks developed during the 26th May 2021 Gisenyi earthquake around Goma and Gisenyi

without pillars or beams. Almost all the buildings were identified to be in the vulnerability class A or B as per the EMS-98 intensity scale. The post-earthquake reconnaissance survey suggests that several houses experienced wall cracking, wall collapse, and boundary wall collapse or cracks, in addition to complete collapse of brick and mud-brick houses in several places (Fig. 5). Most of the houses in Gisenyi Rubavu City were built with brick with a few wood house. During the earthquake, wooden houses were the least damaged, showing only a little twisting.

On the other hand, reinforced concrete buildings presented high levels of damage and large cracks in walls. A detailed analysis to understand the controlling factor for the building damage pattern observed during the earthquake considering the total 300 data sets collected from the field and detailed survey questionnaires was performed (Supplementary Table ST1, Table 2).

The analysis suggests that around 88% of the houses experienced strong shaking, and produced bumping noises. 38% of the houses completely collapsed, around 73% of houses were damaged with 61% of those being heavily damaged and in need of repair before being reoccupied (Fig. 6). During our field survey, people were also asked whether they saw windows, dishes, and other household objects shaking. Approximately 78% of the people responded that they recalled a strong movement of these objects; many objects fell and were broken (Fig. 6). Based on these observations major controlling factors were determined (Fig. 7).

From the statistical analysis, it is observed that 61% of the structural damage and higher reports of shaking were observed at the location situated within the Kivu basin which is composed of volcanic ash/organic-rich soil or basin fill clay-loose sand deposits (Figs. 1b and 7a-b; Ross et al. 2014).

Another crucial factor was observed which had a strong correlation to the amount of damage to buildings was the age of the building (Fig. 7c). Almost 92% of the damaged buildings were constructed several years ago without any earthquake-resistant measures. Considering the shaking and damage pattern observed in the buildings, EMS-98 intensity was evaluated for all the sites. It indicated that the maximum EMS-98 intensity of IX was observed around the Rubavu market and Gisenyi Sector office (Table 2; Supplementary

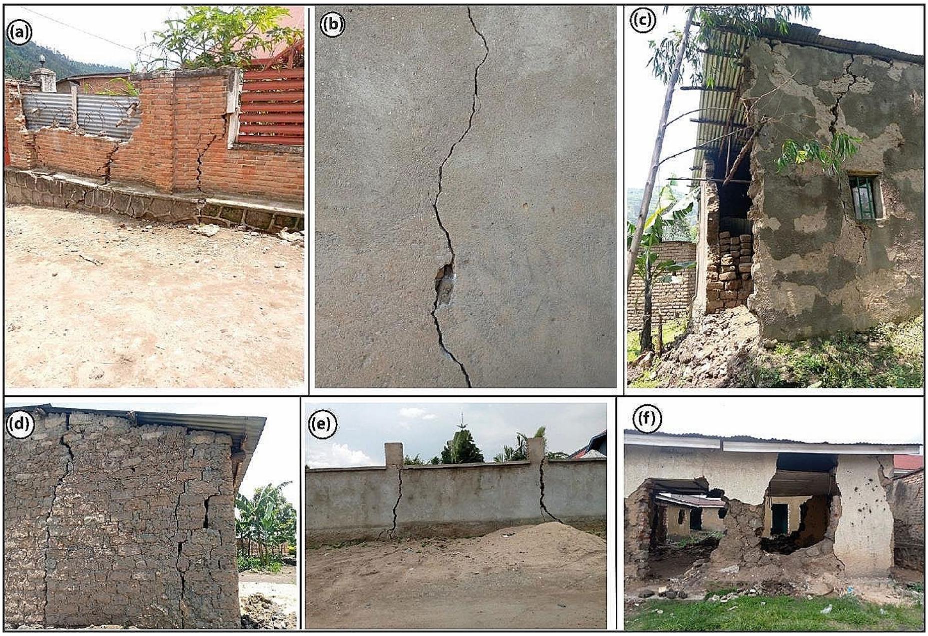

Fig. 5 Typical damage pattern observed in the buildings or fence walls around Gisenyi and Rubavu **a** Umuganda Cell, Gisenyi Sector (Latittude-1.68272°S; Longitude-29.26185°E), **b** Mbugangari Cell, Gisenyi Sector (Latittude-1.67073°S; Longitude-29.26161°E), **c** Gikombe Cell, Rubavu Sector (Latittude-1.66247°S; Longitude-29.28150°E), **d** Rukoko Cell, Rubavu Sector (Latittude-1.66570°S; Longitude-29.254583°E), **e** Amahoro Cell, Gisenyi Sector (Latittude-1.69305°S; Longitude-29.26217°E), **f** Umuganda Cell, Gisenyi Sector(Latittude-1.68846°S; Longitude-29.26200°E)

Table 2 Distribution of EMS-98 intensity and PGA for the selected sites during the 26th May 2021 Gisenyi (Rwanda) Earthquake (Mw 5.1)

Locations	Latitude	Longitude	EMS−98	PGA(g)
College Baptiste Gacuba II	−1.68292	29.26271	VIII	0.41
	−1.68209	29.26210	VII	0.15
Institut Pentecotiste de Gisenyi	−1.68792	29.26195	VIII	0.41
Oscony Construction	−1.68946	29.26220	IX	1.14
Gacuba II B health center	−1.67601	29.25637	VII	0.15
Polycliclinique la Croix du Sud−Gisenyi	−1.69719	29.26161	VII	0.15
Garage Lapide	−1.69100	29.26228	VIII	0.41
Ituze Cell	−1.69190	29.26229	VIII	0.41
	−1.69146	29.26190	IX	1.14
	−1.69257	29.26242	VII	0.15
Cm Jewelry and Boutique	−1.69441	29.26172	VIII	0.41
BK Gisenyi branch	−1.69496	29.26178	VIII	0.41
RRA Office	−1.69042	29.26080	VIII	0.41
Muhabura Mountain Lodge	−1.69647	29.26252	VIII	0.41
Bethany Investment Group	−1.69733	29.26239	VIII	0.41
Tropical Motel	−1.69783	29.26257	IX	1.14
Jerusalem Garden Rubavu	−1.66508	29.25592	VIII	0.41
Gisenyi Cemetery	−1.66309	29.25614	VII	0.15
Byahi Rurembo	−1.66777	29.25547	VII	0.15
Groupe Scolaire Umubano II	−1.66529	29.258028	VII	0.15
Paroisse Muhato	−1.67178	29.263995	VII	0.15
Gisenyi Hospital	−1.69923	29.262431	VIII	0.41
	−1.69719	29.261611	VII	0.15
International School Isoko	−1.70622	29.263159	VII	0.15
Ecole des Science de Gisenyi	−1.70015	29.261664	VII	0.15
Pharmacie du District de Rubavu	−1.70014	29.262525	VII	0.15
Happiness Guest House, Gisenyi	−1.69497	29.259514	IX	1.14
Ecole Secondaire Islamique de Gisenyi	−1.69231	29.258450	VIII	0.41
Centre Scolaire Fraternite	−1.69470	29.25723	VIII	0.41
University of Tourism, Technology and Business Studies (UTB)	−1.66137	29.263599	VII	0.15
ULK Gisenyi	−1.68954	29.25379	VII	0.15
Gisenyi old cemetery	−1.67212	29.26599	VII	0.15
Umubano, Gisenyi	−1.67131	29.25748	VII	0.15
	−1.68146	29.252628	IX	1.14
Mbugangali Market	−1.67624	29.25225	VII	0.15
Byahi Rurembo	−1.66991	29.25232	IX	1.14
Gare routiere	−1.68146	29.25262	IX	1.14
Ubumwe	−1.67578	29.2652	VII	0.15
Gacuba, Gisenyi	−1.67806	29.26434	VII	0.15
Gacuba Primary School	−1.68404	29.26234	VII	0.15
Nest Guest House, Gisenyi	−1.68886	29.26211	VII	0.15
Nengo	−1.72334	29.27095	VII	0.15
Kivu Hilltop View Hotel	−1.73269	29.27623	VII	0.15
Rubavu Port	−1.73526	29.27828	VII	0.15
Rubona	−1.72519	29.26187	VII	0.15

Table 2 (continued)

Locations	Latitude	Longitude	EMS−98	PGA(g)
Groupe Scolaire Rubona, Gisenyi	−1.71348	29.27186	VIII	0.41
Umuganda Stadium	−1.66993	29.26148	VII	0.15
Muhato	−1.67141	29.26114	VII	0.15
	−1.67135	29.26148	IX	1.14
Baptist Secondary School, Gisenyi	−1.67320	29.26296	VII	0.15
ADEPR Gisenyi	−1.68759	29.26198	VIII	0.41
Rugerero	−1.68968	29.27526	VII	0.15
Eglise Adventiste Gisenyi	−1.68277	29.25222	VII	0.15
Heza Beach Resort, Gisenyi	−1.73055	29.26777	VIII	0.41
Sagabay	−1.70694	29.26305	VIII	0.41
Groupe Scolaire Umubano I, Gisenyi	−1.68251	29.25401	VIII	0.41
Agakiriro Rubavu	−1.67654	29.25427	VII	0.15
Buhuru Centre, Gisenyi	−1.66681	29.26273	VII	0.15
Gorillas Lake Kivu Hotel, Gisenyi	−1.69886	29.25597	IX	1.14
Gisenyi Sector Office	−1.69807	29.25676	IX	1.14
	−1.69798	29.2581	VIII	0.41
	−1.698627	29.25761	VII	0.15
Rubavu District Hospital	−1.70191	29.2627	VII	0.15
Ecole Des Science de Gisenyi	−1.69775	29.2612	VIII	0.41
Gisenyi Classic Hop	−1.69441	29.2614	VIII	0.41
BK Gisenyi Branch	−1.6953	29.2618	VIII	0.41
Muhabura Mountain Lodge, Gisenyi	−1.69655	29.2621	VIII	0.41
College Baptiste Gacuba II, Gisenyi	−1.68292	29.26271	VII	0.15
College Baptiste Gacuba II, Gisenyi	−1.68345	29.26247	VII	0.15
Umucyo Christian Center	−1.68709	29.26199	VIII	0.41
Gacuba II Health Center	−1.67692	29.25617	VII	0.15
Gacuba II Health Center	−1.67601	29.25637	VII	0.15
Groupe Scolaire Amahoro, Gisenyi	−1.69496	29.26178	VIII	0.41
Rubavu Mosque	−1.69362	29.26268	IX	1.14
Byahi	−1.66764	29.25774	IX	1.14
Buhuru, Rubavu	−1.66655	29.25950	VIII	0.41
Gisenyi Airport	−1.66999	29.26144	VIII	0.41
	−1.66955	29.25886	VII	0.15
	−1.67888	29.25626	IX	1.14
Centre St Francois D’Assise, Gisenyi	−1.69862	29.25761	VII	0.15
	−1.69862	29.25761	VII	0.15
Rugerero	−1.67178	29.26399	VII	0.15
	−1.69494	29.27004	IX	1.14
	−1.69608	29.26956	VIII	0.41
Rubavu	−1.66075	29.27689	VIII	0.41
	−1.66869	29.25766	VII	0.15
	−1.66897	29.25841	IX	1.14
Centre St Francois D’Assise, Gisenyi	−1.698627	29.25761	VII	0.15
Gisenyi	−1.672127	29.26599	VII	0.15
	−1.69647	29.26252	VIII	0.41
	−1.69146	29.26190	IX	1.14

Table 2 (continued)

Locations	Latitude	Longitude	EMS−98	PGA(g)
Mbungangari Market, Gisenyi	−1.676247	29.25225	VII	0.15

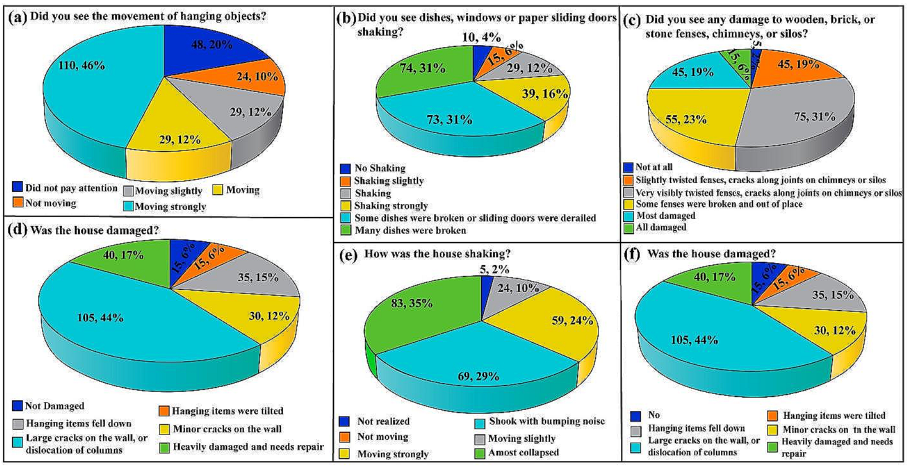

Fig. 6 Pie Charts showing the statistical analysis for the 2023 Gisenyi earthquake shaking effects observed around the study area

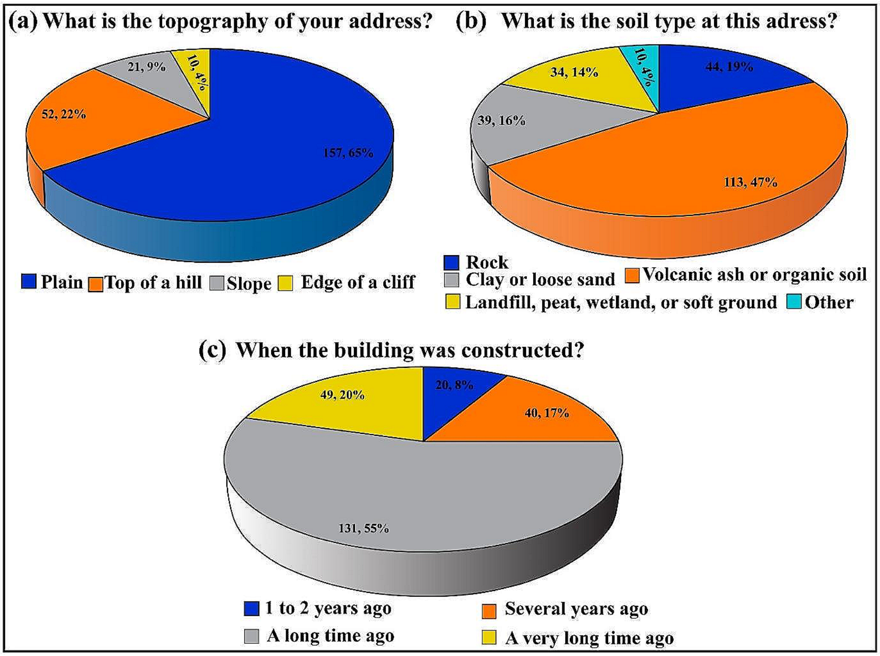

Fig. 7 Pie charts showing the major factors controlling the damage observed during the 26th May 2021 Gisenyi earthquake

Table ST1; Fig. 8a). Similarly, an EMS-98 intensity of VIII was observed around Gisenyi Hospital, Ecole des Sciences de Gisenyi, Mbugangali and Umuganda Cells, Gisenyi airport, and Rugerero Sector. An EMS-98 intensity of VII was also observed around the University of Tourism, Technology and Business Studies (UTB), as well as the Rugerero Sector. From the intensity distribution map, it was noted that the higher intensity values were clustered along the eastern basin-bounding fault of the Kivu rift (Figs. 1 and 8a; Table 2; Supplementary Table ST1).

3.2 Peak ground acceleration (PGA) estimation

Peak ground acceleration (PGA) is the maximum ground acceleration that occurred during the earthquake at a location. PGA is the largest amplitude the accelerogram recorded at a site during a particular earthquake by a seismogram (Musson 2000; Douglas 2003; Douglas et al. 2023). PGA is the most common parameter in engineering applications including ground response analysis, liquefaction potential estimation, seismic building codes design, and seismic hazard maps preparation (Shedlock et al. 2000; Jishnu et al. 2013; Nas et al. 2020; Jena et al. 2021; Naik 2022; Sabetta et al. 2023).

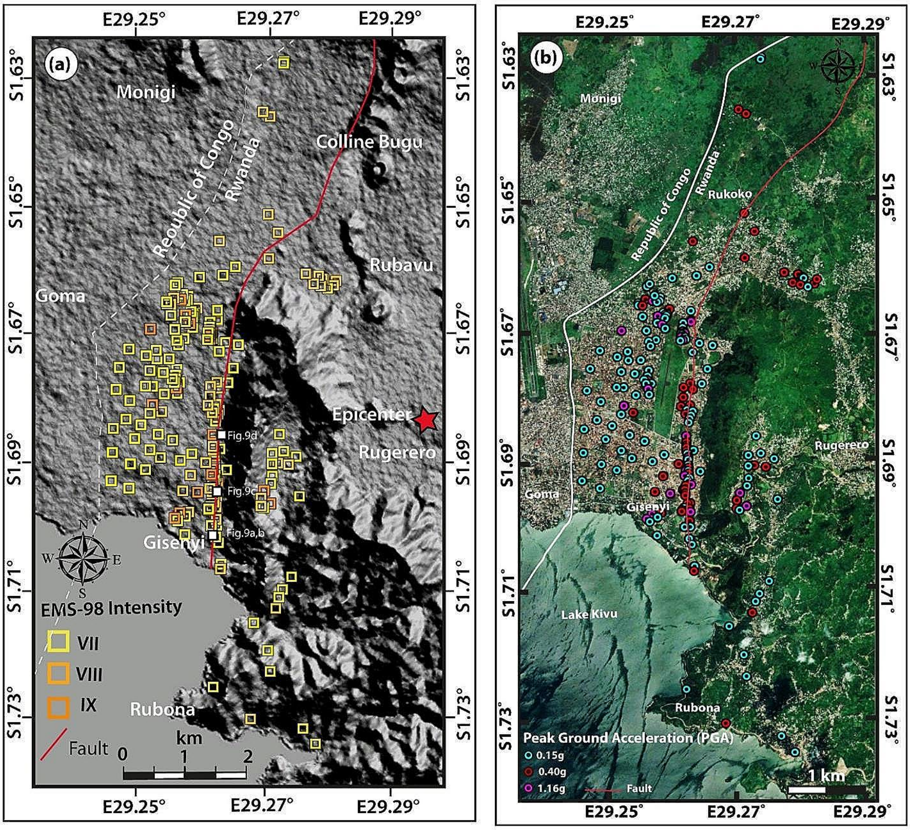

Fig. 8 Map showing **a** the EMS-98 Intensity distribution, **b** Peak Ground Acceleration (PGA) around Gisenyi and Rubavu sectors for the 26th May 2021 Gisenyi earthquake

Therefore, a significant amount of seismic hazard assessment has been carried out with a focus on PGA (Abrahamson 2006; Wang 2011; Nas et al. 2020; Jena et al. 2021; Sabetta et al. 2023). For areas having a higher density of instrumental facilities, the PGA values are be easily available. However, the PGA values can be estimated from macroseismic intensity for areas with limited or no instrumental facility.

Several studies have been carried out to relate seismic intensity to peak ground acceleration (Gutenberg and Richter 1956; Hershberger 1956; Ambraseys 1974; Murphy and O'Brien 1977; McCann et al. 1980; Krinitzsky and Chang 1988; Gama-Garcia and Gómez-Bernal, 2008; Worden et al. 2012; Lesueur et al. 2013; Bilal and Askan 2014; Locati et al. 2017; Du et al. 2019) due to its importance in seismic resistant design (understanding the response of the structures) for future disaster management planning (Bilal and Askan 2014; Du et al. 2019). Nevertheless, most of the correlations are focused on the MM intensity or MCS intensity without any studies focusing on EMS-98 intensity. The relationships between the PGA and intensity are region-specific. Only one or two studies have used EMS-98 intensity to estimate the PGA (Zanini et al. 2019). Since damage pattern and damage level rely on the local scale geological conditions and building vulnerability, local scale studies are required in order to be useful for enhancing the empirical relationship on a regional scale. This can be done by adding more data as well as conducting a local scale seismic hazard analysis. The EMS-98 intensity scale was updated to include earthquake-resistant buildings and to include the most recent traditional intensity scale (Cito et al. 2022; Del Mese et al. 2023). Since there is no such relationship available for the African region, we have utilized an empirical relationship between the EMS-98 intensity and PGA (Eq. 1) as provided by Zanini et al. (2019).

$I_{EMS-98} = 2.03 + 2.28 \times \log PGA$ (1).

Since there are no recording stations around the epicentral area, this formula was used to estimate the peak ground acceleration (PGA), and a PGA distribution map was prepared (Fig. 8b).

PGA values of 1.16 g and 0.40 g were highly concentrated along the eastern basin-bounding faults of the Kivu rift whereas the PGA values of 0.15 g were highly concentrated around the Kivu basin (Fig. 8b). The higher PGA values of 1.16 g and 0.40 g were observed around Rubavu market, Gisenyi Sector office, Gisenyi Hospital, Ecole des Sciences de Gisenyi, Mbugangali and Umuganda Cells, Gisenyi airport, Rugerero area. The PGA values of 0.15 g were mostly composed of volcanic/organic-rich soil around the University of Tourism, Technology and Business Studies (UTB), Rugerero area. In some places, the EMS-98 intensity and PGA values are highly scattered. This may be due to the amalgamation of heterogeneous building types.

In this study, a ShakeMap was produced using the EMS-98 intensity values for the 2021 Gisenyi earthquake using the Earthworm Software Module (Fig. 9). The working principle of the ShakeMap program is based on receiving intensity values from the input file and saving the value of each location. Therefore, from the stored values, the software performs the spatial interpolation calculation using inverse distance weighting to generate a reasonable ShakeMap (Mittal et al. 2019; Wu et al. 2019). This methodology has been applied in many studies (e.g. Legendre et al. 2017; Mittal et al. 2018; Yang et al. 2018, 2021; Naik et al. 2023a; b; Naik et al. 2024). The Gisenyi earthquake ShakeMap shows a maximum intensity of IX around Rubavu with other affected areas showing an intensity of VIII (Fig. 9). The intensity map is the first ShakeMap made available for the 26th May 2021 Mw 5.1

earthquake. There is no other such map available for the earthquake at the moment. The ShakeMap does not depict the entirety of the damaged area io due to the non-availability of the data from the DR Congo part. However, the ShakeMap presented here (Fig. 9) can be used for to improve seismic hazard estimation, land use, and land cover planning for the affected area, more specifically for the Goma, Gisyenyi, and Rubavu regions, in the future.

4 Discussions

Detailed field reconnaissance surveys were performed around the Rugerero, Gisenyi, and Rubavu Sectors of Rubavu District, Rwanda, which were highly affected by the 26th May 2021 Gisenyi earthquake (M_w 5.1). The Gisenyi earthquake (M_w 5.1) caused extensive shaking and damage around the Gisenyi and Rubavu sectors of Rwanda. Although the earthquake caused shaking and building damage in the DR Congo, due to international border issues we were not able to conduct a field survey in DR Congo.

Around 300 data sets were collected through macrosiemsic survey questionnaires and field surveys, then EMS-98 intensity values were assigned for each location. The EMS-98 values suggest a maximum intensity of IX for the M_W, 26th May 2021 Gisenyi earthquake (Fig. 8a). Higher intensity values were observed in urban areas with higher population densities in the Rugerero, Gisenyi, and Rubavu Sectors. We have prepared a seismic intensity distribution map which is the first one created for this earthquake. We estimated PGA values using the EMS-98 intensity and also prepared a PGA distribution map (Fig. 8b) which can be used for future seismic hazard assessment and earthquake-resistant building design. Despite the moderate magnitude, the earthquake produced higher seismic intensity effects due to the lack of earthquake resistant design and nonexistent building regulations in Rwanda. This led to the construction of masonry buildings in the city of Gisenyi, which are unstable and very susceptible to earthquakes (Figs. 3 and 5).

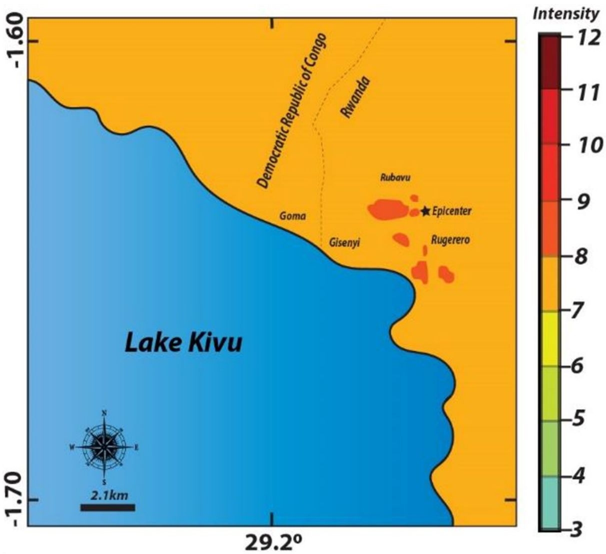

Fig. 9 EMS-98 ShakeMap for the 26th May 2021 Gisenyi earthquake prepared from the field-based building damage data

In addition to this, several other factors such as the age of the buildings, non-ductile detailing of structural components, strong-beam weak-column conditions, captive-column and short-column effects, soft and weak stories mechanism, irregularity in plan and elevation, local geology, unconfined infill walls, bad workmanship, low quality of construction materials, superficial detailing of building elements, and the lack of engineering services contributed to the severity of the damage (Ademović et al. 2020; Alih and Vafaei 2019; Günaydin et al. 2021). Most of the damaged buildings were located along the volcanic/organic-rich soil or soil having a higher percentage of sand and silt. This might indicate site amplification (Joshi et al. 2023) and suggests a proper geotechnical characterization is required of the soil to understand its seismic response for a better seismic hazard assessment of the area.

The macroseismic intensity values we reported are similar to those observed in several earthquakes of moderate magnitude in various seismotectonic contexts. In volcanic regions, these intensity values are attributed to factors such as the shallow depth of the earthquake's hypocenter, the superficial nature of the seismogenic source, the inferior quality of surface deposits, and inadequate construction practices, as highlighted by Nappi et al. (2021) and Tringali et al. (2023). Comparable intensity values have also been recorded for several moderate-magnitude earthquakes worldwide. In active tectonic areas, such as Romania which was hit by the 2004 Vracea earthquake (Mw 6.0) (Constantin et al. 2016), India (Haryana Delhi border) which was hit by a 2012 earthquake (Mw 4.9) (Gupta et al. 2013), Albania which was hit by a 2019 Durres earthquake (Mw 5.6) (Rrezart and Rrapo, 2020), Grecia (West Athens) which was hit by a 2019 earthquake (Mw 5.1) (Kouskouna et al. 2021), Italy which was hit by the 2012 Emilia Romagna seismic sequence, (Mw 5.9) (e.g. Tertulliani et al. 2012), the 2017 Casamicciola earthquake (M_W 3.9) (Nappi et al. 2021) and the 2018 Fleri earthquake (Mw 4.9) (Tringali et al. 2023).

During the field survey and macroseismic reconnaissance survey, it was observed that most of the wooden buildings resisted the earthquake. Only minor cracks were observed in the wall (Figs. 5 and 10). Although the wooden structures in Rwanda are not properly designed as per the seismic building code, they had the flexible properties of wooden materials, high strength-to-weight ratio, and lightweight the structure, which allow them to withstand the seismic waves passing through them either without breaking or just the development of minor cracks or damage (Kaushik et al. 2006; Buchanan et al. 2011a, b; Alih and Vafaei 2019). The better performance of wooden buildings was also observed during several moderate magnitude earthquakes such as the 2006 Sikkim earthquake in India (M_w 5.3; Kaushik et al. 2006); the 2010 Elazığ-Kovancılar earthquake in Turkey (M_W 6.1; Calayır et al. 2012), the 2011 Christchurch earthquake in New Zealand (M_w 6.3; Buchanan et al. 2011a), and the 2015 Mw 6.0 Sabah earthquake in Malaysia (Mw 6.0; Alih and Vafaei 2019). Considering the shaking intensity, building damage pattern observed in different types of buildings, and the macroseismic intensity calculated from our analysis (Table 2; Supplementary Table ST1), it is recommended that seismic design codes be implemented to prevent the reoccurrence of such damage in the future.

The ShakeMap for the 2021 Gisenyi earthquake (Fig. 9) shows a concentration of higher intensity (IX) around the probable surface rupture and lower intensity (EMS-98-VIII) in other areas. A Higher intensity might also be predicted close to the epicenter (Naik et al. 2023b), however unlike the basin, the affected area is hilly terrain and consists of Meso-Proterozoic rocks. This is indicative of the effect that local geology has on shaking intensity

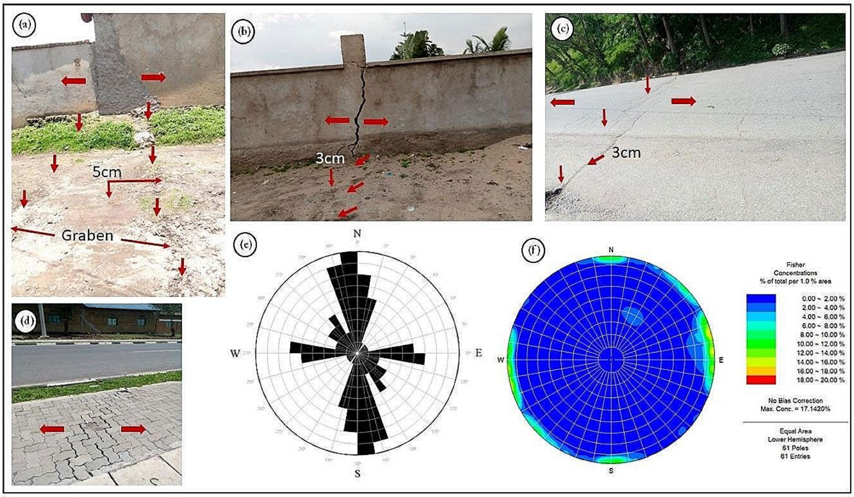

Fig. 10 Field photo graphs showing (**a**) extensional graben with 5 cm vertical displacement along the Eastern Basin Boundary fault, (**b**) extensional cracks along the boundary wall and its adjacent ground with 3 cm vertical displacement, (**c**) extensional ground cracks observed on road with 3 cm vertical displacement, (**d**) extensional cracks and opening in the pedestrians, (**e**) and (**f**) Stereo plot showing the orientation of the extensional cracks observed during the earthquakes along the Eastern Basin Boundary fault, Kivu Rift

and the macroseismic intensity calculated from our analysis (Table 2, Supplementary Table ST1).

The ShakeMap prepared from the present study can be used for better seismic hazard estimation of Gisenyi City. This is the first-time damaged-based field data were used for the ShakeMap generation of the affected area. The field data-based ShakeMap represents a more accurate hazard scenario than a ShakeMap prepared from the instrumental records for the areas due to having limited or no near source seismic monitoring stations (Musson 2000; Silva et al. 2017; Cito et al. 2022; Naik et al. 2023a, b; Bhochhibhoya and Maharjan 2022; Trevlopoulos et al. 2023).

In addition, the clustering of higher intensity values, higher PGA values, and higher grades of damaged buildings along the eastern boundary of the Kivu basin might be related to the reactivation of the eastern basin-bounding fault. Furthermore, it could be associated with the acceleration of ground motion close to the fault, source directivity, and site effects (Figs. 1 and 10a-b; Mollaioli et al. 2006; Pacor et al. 2018). The reactivation could be associated with the diking process or regional extension. Although a more detailed structural analysis is required for testing these two hypothetical causes, our field survey results suggested it was the reactivation of the eastern boundary fault based on the structural parameters collected from the earthquake-induced fracture pattern observed along the eastern boundary fault (Figs. 1a-b and 10). Most of the extensional fractures show a vertical displacement of 3–5 cm (Figs. 4b-d and 10a-d), and they predominantly indicate N-S/NNE-SSW strikes similar to the trend along the eastern basin-bounding fault (Fig. 10e-f).

Similar phenomena of higher seismic intensity due to the fault reactivation were observed during the 1999 Chi-Chi earthquake (Xie 2019), the 2003 Bingöl earthquake in Turkey

(Akkar et al. 2005), the 2008 Wenchuan earthquake (Xie et al. 2010), the 2011 Tohoku earthquake in Japan (Pavlenko 2022), 2013 Cook Strait earthquake in New Zealand (Holden et al. 2013), and the 2011 Christchurch earthquake in New Zealand (Bradley 2016).

The present study can be utilized as an initial step toward a better understanding of the seismic hazard potential of the area. The presented EMS-98 intensity and PGA distribution map is vital for better seismic hazard estimation, land use, and land cover planning for the affected area in the future.

5 Conclusions

EMS-98 intensity and PGA values were estimated for the 26th May 2021 Gisenyi earthquake (M_w 5.1). We determined a maximum intensity Imax = IX to the 2021 Gisenyi earthquake. From the seismic intensity survey, it can be inferred that the buildings located in volcanic soil/organic-rich soil are prone to higher seismic damage. In addition, despite of similar construction method material, older buildings suffered a higher degree of damage. Therefore, there is an urgent requirement for the implementation of a seismic design code in the construction of both modern as well as traditional buildings in Rwanda.

The higher intensity and PGA values were concentrated along N-S/NNE-SSW, which is a similar trend to the eastern boundary fault of the Kivu rift, indicating the direction of rupture propagation.

The prepared EMS-98 and PGA map can be applicable for future seismic hazard assessment and implementation of building codes in the affected region.

Finally, this research concludes that analyses of earthquake-induced damage data can help to identify hazard scenarios, shaking intensity and develop knowledge that is useful to formulate new disaster risk reduction policies in Rwanda which does not have any previous seismic hazard zonation or risk studies.

Supplementary Information The online version contains supplementary material available at https://doi.org/10.1007/s11069-024-06637-7.

Acknowledgements This research was supported by a grant(2022-MOIS62-001(RS-2022-ND640011)) of National Disaster Risk Analysis and Management Technology in Earthquake funded by the Ministry of Interior and Safety (MOIS, Korea).

Declarations

Conflict of interest The authors have no relevant financial or non-financial interests to disclose about the research.

References

Abrahamczyk L, Lang DH, Schwarz J (2017) WHE-reports as a complementary database towards the development of an international macroseismic scale. In 16th World Conference on Earthquake Engineering, Santiago, Chile

Abrahamson NA (2006) Seismic hazard assessment: problems with current practice and future developments. In First European Conference on Earthquake Engineering and Seismology. pp 3–8

Ademović N, Hadzima-Nyarko M, Zagora N (2020) Seismic vulnerability assessment of masonry buildings in Banja Luka and Sarajevo (Bosnia and Herzegovina) using the macroseismic model. Bull Earthq Eng 18:3897–3933. https://doi.org/10.1007/s10518-020-00846-8

Akkar S, Boore DM, Gülkan P (2005) An evaluation of the strong ground motion recorded during the May 1, 2003, Bingöl Turkey, Earthquake. J Earthq Eng 9(2):173–197

Alih SC, Vafaei M (2019) Performance of reinforced concrete buildings and wooden structures during the 2015 mw 6.0 Sabah earthquake in Malaysia. Eng Fail Anal 102:351–368. https://doi.org/10.1016/j.engfailanal.2019.04.056

Allen TI, Wald DJ, Earle PS, Marano KD, Hotovec AJ, Lin K, Hearne MG (2009) An Atlas of ShakeMaps and population exposure catalog for earthquake loss modeling. Bull Earthq Eng 7:701–718

Ambraseys NN (1974) The correlation of intensity with ground motion. Proc. 14th Conference of European Seismological Communication, Trieste, Italy 1:335–341

Azzaro R, Ferreli L, Michetti AM, Serva L, Vittori E (1998) Environmental hazard of capable faults: the case of the Pernicana Fault (Mt. Etna, Sicily). Nat Haz 17(2):147–162

Azzaro R (1999) Earthquake surface faulting at Mount Etna volcano (Sicily) and implications for active tectonics. J Geodyn 28(2-3):193–213

Azzaro R, Bella D, Ferreli L, Michetti AM, Santagati F, Serva L, Vittori E (2000) First study of fault trench stratigraphy at Mt. Etna volcano, Southern Italy: understanding Holocene surface faulting along the Moscarello fault. J Geodyn 29(3-5):187–210

Azzaro R, D'Amico S, Tuvè T (2011) Estimating the magnitude of historical earthquakes from macroseismic intensity data: new relationships for the volcanic region of Mount Etna (Italy). Seismol Res Lett 82(4):533–544

Barth A, Wenzel F, Giardini D (2007) Frequency sensitive moment tensor inversion for light to moderate magnitude earthquakes in eastern Africa. Geophy Res Lett 34(15):L15302

Bhochhibhoya S, Maharjan R (2022) Integrated seismic risk assessment in Nepal. Nat Hazards Earth Syst Sci 22(10):3211–3230

Bilal M, Askan A (2014) Relationships between felt intensity and recorded ground-motion parameters for Turkey. Bull Seismol Soc Am 104(1):484–496

Boudoire G, Calabrese S, Colacicco A, Sordini P, Habakaramo Macumu P, Rafflin V, Valade S, Mweze T, Kazadi Mwepu JC, Safari Habari F, Amani Kahamire T (2022) Scientific response to the 2021 eruption of Nyiragongo based on the implementation of a participatory monitoring system. Sci Rep May 6;12(1):7488

Bradley BA (2016) Strong ground motion characteristics observed in the 13 June 2011 Mw6.0 Christchurch, New Zealand earthquake. Soil Dyn Earthq Eng 91:23–38

Buchanan AH, Bull D, Dhakal R, MacRae G, Palermo A, Pampanin S (2011a) Base isolation and damage-resistant technologies for improved seismic performance of buildings: A report written for the Royal Commission of Inquiry into building failure caused by the Canterbury earthquakes. Department of Civil and Natural Resources Engineering, University of Canterbury; 2011.DOC ID: ENG.ACA.0010.FINAL.

Buchanan A, Carradine D, Beattie G, Morris H (2011b) Performance of houses during the Christchurch earthquake of 22 February 2011. Bull N Z Soc Earthq Eng 44(4):342–357

Buforn E, Udías A (2022) The 1620 and 1644 earthquakes in Alcoy and the eastern region of Spain. Seismol Res Lett 93:2335–2346. https://doi.org/10.1785/0220220053

Calayır Y, Sayın E, Yön B (2012) Performance of structures in the rural area during the March 8, 2010 Elazığ-Kovancılar earthquake. Nat Hazards 61:703–717. https://doi.org/10.1007/s11069-011-0056-6

Cito P, Chioccarelli E, Iervolino I (2022) Macroseismic intensity hazard maps for Italy based on a recent grid source model. Bull Earthq Eng 20(5):2245–2258

Constantin AP, Moldovan IA, Craiu A, Radulian M, Ionescu C (2016) Macroseismic intensity investigation of the November 2014, M = 5.7, Vrancea (Romania) crustal earthquake. Ann Geophys 59(5):S0542–S0542

Contreras D, Wilkinson S, James P (2021) Earthquake reconnaissance data sources, a literature review. Earth 2(4):1006–1037

Cornet J (1910) Sur la repartition des tremblements de terre dans le bassin du Congo. Ann Soc Geol Belg 36:B264–B269 (1908–1909)

CS.LL.PP (2018) Aggiornamento delle norme tecniche per le costruzioni. Gazz Ufficiale Della Repubblica Italiana 42. (In Italian.)

Cua G, Wald DJ, Allen TI, Garcia D, Worden CB, Gerstenberger M, Lin K, Marano K (2010) Best practices for using macroseismic intensity and ground motion intensity conversion equations for hazard and loss models in GEM1 (p. 4). GEM Technical Report 2010-4, GEM Foundation, Pavia, Italy. www.globalquakemodel.org

d'Oreye N, Gonzalez P, Shuler A, Oth A, Bagalwa M, Ekström G, Kavotha D, Kervyn F, Lucas C, Lukaya F, Osodundu E, Wauthier C, Fernandez J (2011) Source parameters of the 2008 Bukavu-Cyangugu earthquake estimated from InSAR 1168 and teleseismic data. Geophys J Int 184(2):934–948

Del Mese S, Graziani L, Meroni F, Pessina V, Tertulliani A (2023) Considerations on using MCS and EMS-98 macroseismic scales for the intensity assessment of contemporary Italian earthquakes. Bull Earthq Eng :1–23

Delvaux D, Barth A (2010) African stress pattern from formal inversion of focal mechanism data. Implications for rifting dynamics. Tectonophysics 482:105–128

Delvaux D, Mulumba JL, Sebagenzi MNS, Bondo SF, Kervyn F, Havenith HB (2017) Seismic hazard assessment of the Kivu rift segment based on a new seismotectonic zonation model (western branch, east African rift system). J Afr Earth Sci 134:831–855

Dengler L, McPherson R (1993) The 17th August 1991 Honeydaw earthquake, north coast California: a case for revising the modified mercalli scale in sparsely populated areas. Bull Seismol Soc Am 83:1081–1094

Douglas J (2003) Earthquake ground motion estimation using strong-motion records: a review of equations for the estimation of peak ground acceleration and response spectral ordinates (PDF). Earth Sci Rev 61(1–2):43–104

Douglas J, Crowley H, Silva V, Marzocchi W, Danciu L, Pinho R (2023) Methods for evaluating the significance and importance of differences amongst probabilistic seismic hazard results for engineering and risk analyses: a review and insights, EGU sphere [preprint] 2023 – 991. https://doi.org/10.5194/egusphere

Du K, Ding B, Luo H, Sun J (2019) Relationship between peak ground acceleration, peak ground velocity, and macroseismic intensity in Western China. Bull Seismo Soc Am 109(1):284–297

Earle PS, Wald DJ, Jaiswal KS, Allen TI, Hearne MG, Marano KD, Hotovec AJ, Fee JM (2009) Prompt Assessment of global earthquakes for response (PAGER): a system for rapidly determining the impact of earthquakes worldwide. US Geol Surv Open-File Rep 1131:15. https://doi.org/10.3133/ofr20091131

Esposito E, Porfido S, Mastrolorenzo G, Nikonov AA, Serva L (1997) Brief review and preliminary proposal for the use of ground effects in the macroseismic intensity assessment. In: Proceedings of the 30th International Geological Congress, Beijing, China, 5p. Contemporary Lithospheric Motion Seismic Geology, International Science Publishers, Zeist, The Netherlands 233–243

Faenza L, Michelini A (2010) Regression analysis of MCS intensity and ground motion parameters in Italy and its application in ShakeMap. Geophys J Int 180(3):1138–1152

Ferreli L, Michetti AL, Serva L, Vittori E (2002) Stratigraphic evidence of coseismic faulting and aseismic fault creep from exploratory trenches at Mt. Etna volcano (Sicily, Italy). Geol Soc Ame Bull 359:49–62

Galea P (2007) Seismic history of the Maltese islands and considerations on seismic risk. Ann Geophys. https://doi.org/10

Gama-Garcia A, Gómez-Bernal A (2008) Relationships between instrumental ground motion parameters and modified Mercalli intensity in Guerrero, Mexico, 14th World Conf. on Earthquake Engineering, Beijing, China, 13–17 October 2008

Geirsson H, d'Oreye N, Mashagiro N, Syauswa M, Celli G, Kadufu B, Smets B, Kervyn F (2017) Volcano-tectonic deformation in the Kivu Region, Central Africa: results from six years of continuous GNSS observations of the Kivu Geodetic Network (KivuGNet). J Afr Earth Sci 134:809–823

Giovinazzi S, Lagomarsino S (2004) A macroseismic model for the vulnerability assessment of buildings. In: Proc. 13th world conference on earthquake engineering. Vancouver, Canada, paper 896 (CD-Rom)

Gomez-Capera AA, D'Amico M, Lanzano G, Locati M, Santulin M (2020) Relationships between ground motion parameters and macroseismic intensity for Italy. Bull Earthq Eng 18:5143–5164. https://doi.org/10.1007/s10518-020-00905-0

Grunthal G (1998) European Macroseismic Scale 1998 (EMS-98). European Seismological Commission, Subcommission on Engineering Seismology, Working Group Macroseismic Scales. Conseil de l'Europe, Cahiers du Centre Europe´en de Ge´odynamique et de Se´ismologie 15:99

Günaydin M, Atmaca B, Demir S, Altunişik AC, Hüsem M, Adanur S, Ateş Ş, Angin Z (2021) Seismic damage assessment of masonry buildings in Elazığ and Malatya following the 2020 Elazığ-Sivrice earthquake, Turkey. Bull Earthq Eng 19:2421–2456

Gupta AK, Chopra S, Prajapati SK, Sutar AK, Bansal BK (2013) Intensity distribution of M 4.9 Haryana–Delhi border earthquake. Nat Hazards 68:405–417

Gutenberg B, Richter CF (1956) Earthquake magnitude, intensity, energy, and acceleration. Bull Seismol Soc Am 46(2):105–145

Hamaguchi H, Nishimura T, Zana N (1992) Process of the 1977 Nyiragongo eruption inferred from the analysis of long-period earthquakes and volcanic tremors. Tectonophysics 209(1–4):241–254

Hershberger J (1956) A comparison of earthquake accelerations with intensity rating. Bull Seismol Soc Am 46(4):317–320

Holden C, Kaiser A, Van Dissen R, Jury R (2013) Sources, ground motion and structural response characteristics in Wellington of the 2013 Cook Strait earthquakes. Bull N Z Soc Earthq Eng 46(4):188–195

Jena R, Naik SP, Pradhan B, Beydoun G, Park HJ, Alamri A (2021) Earthquake vulnerability assessment for the Indian subcontinent using the long short-term memory model (LSTM). Int J Disaster Risk Reduct 66:102642

Jishnu RB, Naik SP, Patra NR, Malik JN (2013) Ground response analysis of Kanpur soil along Indo-Gangetic Plains. Soil Dyn Earthq Eng 51:47–57

Joshi M, Naik SP, Mohanty A, Bhadran A, Girishbai D, Ghosh S (2023) First-hand observations from the April 28, 2021 Sonitpur (MW 6.4) earthquake, Assam, India: possible mechanism involved in the occurrence of widespread ground effects. Geosci J 27:225–239. https://doi.org/10.1007/s12303-022-0032-z

Kamer Y, Abdulhamitbilal E, Demircioglu MB, Erdik M, Hancilar U, Sesetyan K, Zulfikar AC (2009) Earthquake loss estimation routine ELER v. 1.0 user manual. Bogazici University, Department of Earthquake Engineering, Istanbul Turkey

Kasahara M, Tanaka K, Zana N (1991) A flank eruption of volcano Nyamuragira in 1991: Mikombe. J Afr Stud 39:29–50

Kaushik HB, Durgesh CR, Sudhir KJ (2006) Code approaches to seismic design of masonry-infilled reinforced concrete frames: a state-of-the-art review. Earthq Spectra 22(4):961–983

Komorowski1 J-C, Tedesco D, Kasereka M, Allard P, Papale P, Vaselli O, Durieux J, Baxter P, Halbwachs M, Akumbe M, Baluku B, Briole P, Ciraba M, Dupin JC, Etoy O, Garcin D, Hamaguchi H, Houlié N, Kavotha KS, Lemarchand A, Lockwood J, Lukaya N, Mavonga G, de Michele M, Mpore S, Mukambilwa K, Munyololo F, Newhall C, Ruch J, Yalire M, Wafula M (2002/2003) The January 2002 flank eruption of Nyiragongo volcano (Democratic Republic of Congo): chronology, evidence for a tectonic trigger, and impact of lava flows on the city of Goma, in Acta Vulcanologica, 14(1–2) and Istituti Editoriali e Poligrafici Internazionali, Pisa–Roma 15(1–2):27–61

Kouskouna V, Ganas A, Kleanthi M, Kassaras I, Sakellariou N, Sakkas G, Bossu R (2021) Evaluation of macroseismic intensity, strong ground motion pattern, and fault model of the 19 July 2019 Mw5. 1 earthquake west of Athens. J Seismol 25:747–769

Krenkel E (1922) Die Bruchzonen Ostafrikas: Tectonik, Vulkanismus, Erdbeben and Schwere Anomalien., Berlin

Krinitzsky EL, Chang FK (1988) Intensity-related earthquake ground motion. Bull Int Assoc Eng Geol 4:425–435

Legendre CP, Tseng TL, Mittal H, Hsu CH, Karakhanyan A, Huang BS (2017) Complex wave propagation revealed by peak ground velocity maps in the Caucasus Area. Seis Res Let 88(3):812–821

Lesueur C, Cara M, Scotti O, Schlupp A, Sira C (2013) Linking ground motion measurements and macroseismic observations in France: a case study based on accelerometric and macroseismic databases. J Seismol 17:313–333. https://doi.org/10.1007/s10950-129-3192

Li Q, Shi Y, Huang X, Zhu XX (2020) Building footprint generation by integrating convolution neural network with feature pairwise conditional random field (FPCRF). In: IEEE Trans Geosci Remote Sens (1–18)

Locati M, Capera AA, Puglia R, Santulin M (2017) Rosetta, a tool for linking accelerometric recordings and macroseismic observations: description and applications. Bull Earthq Eng 15:2429–2443. https://doi.org/10.1007/s10518-016-9955-y

Martin SS, Cummins PR, Meltzner AJ (2022) Gempa Nusantara: a database of 7380 macroseismic observations for 1200 historical earthquakes in Indonesia from 1546 to 1950. Bull Seism Soc Am 112:2958–2980. https://doi.org/10.1785/0120220047

Mavonga T (2007) An estimate of the attenuation relationship for the strong ground motion in the Kivu Province, Western Rift Valley of Africa. Phys Earth Planet Int 62:13–21

Mavonga T, Durrheim RJ (2009) Probabilistic seismic hazard assessment for the Democratic Republic of Congo and surrounding areas. South Afr J Geol 209:329–342

McCann MW, Sauter JF, Shah HC (1980) A technical note on PGA-intensity relations with applications to damage estimation. Bull Seismol Soc Am 70(2):631–637

Michelini A, Faenza L, Lanzano G, Lauciani V, Jozinovic D, Puglia R, Luzi L (2019) The new ShakeMap in Italy: progress and advances in the last 10 yr. Seismol Res Lett 91(1):317–333

Michetti AM, Esposito E, Gu¨rpinar J, Mohammadioun B, Mohammadioun A, Porfido S, Rogozhin E, Serva L, Tatevossian R, Vittori E, Audemard F, Comerci V, Marco S, McCalpin J, Mo¨rner NA (2004) The INQUA Scale. An innovative approach for assessing earthquake intensities based on seismically-induced ground effects in the natural environment. In: Vittori, E, Comerci, V, (Eds.), Special Paper, Agenzia nazionale per la protezione dell'ambiente e per i servizi tecnici, Memorie Descrittive della Carta Geologica d'Italia 68:1–120

Michetti AL, Audemard F, Azuma T, Clague J, Comerci V, Esposito E, Guerrieri L, Grpinar A, McCalpin J, Mohammadioun B, Morner NA, Ota Y, Roghozin E (2007) Intensity scale ESI 2007. In: Guerrieri L, Vittori E (eds) Memorie Descrittive Carta Geologica d'Italia. Servizio Geologico d'Italia, vol. 74, Dipartimento Difesa del Suolo, APAT, Roma, p 53

Mittal H, Wu YM, Sharma ML, Lin TL, Yang BM (2018) Shake maps generation for Delhi region using two different algorithms. In: Proceedings of the 16th Symposium on Earthquake Engineering. Department of Earthquake Engineering, Indian Institute of Technology, Roorkee, India 20–22

Mittal H, Wu YM, Lin TL, Legendre CP, Gupta S, Yang BM (2019) Time-dependent ShakeMaps map for Uttarakhand Himalayas, India, using recorded earthquakes. Act Geophy 67:753–763. https://doi.org/10.1007/s11600-019-00281-7

Mollaioli F, Bruno S, Decanini LD, Panza GF (2006) Characterization of the dynamic response of structures to damaging pulse-type near-fault ground motions. Meccanica 41:2346. https://doi.org/10.1007/s11012-005-7965-y

Murphy JR, O'Brien LJ (1977) The correlation of peak ground acceleration amplitude with seismic intensity and other physical parameters. Bull Seismol Soc Am 67:877–915

Musson RMW (2000) Intensity-based seismic risk assessment. Soil Dyn Earthq Eng 20:353–360

Musson RM, Grünthal G, Stucchi M (2010) The comparison of macroseismic intensity scales. J Seismol 14:413–428

Naik SP, Mohanty A, Porfido S, Tuttle M, Gwon O, Kim YS (2020) Intensity estimation for the 2001 Bhuj earthquake, India on ESI-07 scale and comparison with historical 16th June 1819 Allah Bund earthquake: a test of ESI-07 application for intraplate earthquakes. Quat Int 536:127–143

Naik SP (2022) Seismic wave amplification and localized ground effects: a geological tool for future land use code and land use planning in the low seismic area in recent developments in using seismic waves as a probe for subsurface investigations. CRC Press, Taylor and Francis Publication, pp 113–132

Naik SP, Mohanty A, Mittal H, Porfido S, Michetti AM, Yang BM, Gwon O, Kim YS (2023a) The earthquake environmental effects (EEEs) of the 6th February 2018, Hualien earthquake (Mw = 6.4): a contribution to the seismic hazard estimation in the epicentral area. Quat Int 656:48–69

Naik SP, Mohanty A, Sotiris V, Mittal H, Porfido S, Michetti AM, Gwon O, Park K, Jaya A, Paulik R, Li C (2023b) 28th September 2018 Mw 7.5 Sulawesi Supershear Earthquake, Indonesia: Ground effects and macroseismic intensity estimation using ESI-2007 scale. Eng Geol 317:107054

Naik SP, Rimando JM, Mittal H, Rimando RE, Porfido S, Kim YS (2024) Reappraisal of the 2012 magnitude (MW) 6.7 Negros Oriental (Philippines) earthquake intensity and ShakeMap generation by using ESI-2007 environmental effects. Geom Nat Haz Ris 15(1):2311890

Nappi R, Alessio G, Gaudiosi G, Nave R, Marotta E, Siniscalchi V, Civico R, Pizzimenti L, Peluso R, Belviso P, Porfido S (2018) The 21 August 2017 MD 4.0 Casamicciola earthquake: first evidence of coseismic normal surface faulting at the Ischia volcanic island. Seism Res Let 89(4):1323–1334

Nappi R, Porfido S, Paganini E, Vezzoli L, Ferrario MF, Gaudiosi G, Michetti AM (2021) The 2017, MD = 4.0, Casamicciola earthquake: ESI-07 scale evaluation and implications for the source model. Geosciences 11(2):44

Nas M, Lyubushin A, Softa M, Bayrak Y (2020) Comparative PGA-driven probabilistic seismic hazard assessment (PSHA) of Turkey with a Bayesian perspective. J Seismol 24:1109–1129. https://doi.org/10.1007/s10950-020-09940-5

Pacor F, Felicetta C, Lanzano G, Sgobba S, Puglia R, D'Amico M, Russo E, Baltzopoulos G, Iervolino I (2018) NESS1: a worldwide collection of strong-motion data to investigate near-source effects. Seismol Res Lett 89(6):2299–2313

Passau G (1911) Tremblements De Terre Au Congo Belge (1909–1910). Bull Soc Geol Belg 37:B215

Passau G (1912) Tremblements De Terre Au Congo Belge (1910–1911). Ann Soc Geol Belg Pub Rel Congo Belge, Annexe Au tome 39 des annales fasc. 1:3–4 (1911–1912)

Pavlenko OV (2022) Influence of source directivity and site effects of 2003 Tokachi-Oki earthquake on the generation of high PGA in the near-fault zones. Sci Rep 12(1):12134

Porfido S, Esposito E, Guerrieri L, Vittori E, Tranfaglia G, Pece R (2007) Seismically induced ground effects of the 1805, 1930, and 1980 earthquakes in the Southern Apennines, Italy. Boll Soc Geol It 126:333–346

Ross KA, Smets B, De Batist M, Hilbe M, Schmid M, Anselmetti FS (2014) Lake-level rise in the late Pleistocene and active subaquatic volcanism since the Holocene in Lake Kivu, East African Rift. Geomorphology 221:274–285

Rrezart BOZO and ORMENİ R (2020) Evaluation of Macroseismic Field of 21 September 2019, Durres Earthquake in Albania. J Int Environ Appl Sci 15(3):181–187

Sabetta F, Fiorentino G, Bocchi F, Sinibaldi M, Falcone G, Mendicelli A (2023) Influence of local site effects on seismic risk maps and ranking of Italian municipalities. Bull Earthq Eng 21(5):2441–2468

Sarabia Gómez AM, Barbosa Castro DR, Arcila Rivera MM (2022) Macroseismic intensity data and effects of significant earthquakes in Colombia based on historical seismicity studies. https://doi.org/10.32685/0120-1425/bol.geol.48.2.2021.638. Bol geol

Saria E, Calais E, Stamps DS, Delvaux D, Hartnady CJH (2014) Present-day kinematics of the East African Rift. J Geophys Res Solid Earth 119(4):3584–3600

Serva L (1994) Ground effects in intensity scales. Terra Nova 6:414–416

Shedlock KM, Giardini D, Grunthal G, Zhang P (2000) The GSHAP global seismic hazard map. Seismol Res Lett 71(6):679–686

Sibol MS, Bollinger GA, Birch B (1987) Estimation of magnitudes in central and eastern North America using intensity and felt area. Bull Seismol Soc Am 77:1635–1654

Sieberg A (1932) Die erdbeben. In: Gutenberg, B. (Ed.), Handbuch der geophysik. Bonrntrager, Berlin 4:188–191

Silva PG, Horspool N (2019) Combining USGS ShakeMaps and the OpenQuake-engine for damage and loss assessment. Earthq Eng Struct Dyn 48(6):634–652

Silva PG, Elez J, Giner-Robles JL, Rodríguez-Pascua MA, Pérez-López R, Roquero E, Bardají T, Martínez-Graña A (2017) ESI-07 ShakeMaps for instrumental and historical events in the Betic Cordillera (SE Spain): an approach based on geological data and applied to seismic hazard. Quat Int 451:185–208

Silveira D, Gaspar JL, Ferreira T, Queiroz G (2003) Reassessment of the historical seismic activity with major impact on S. Miguel Island (Azores). Nat Hazards Earth Syst Sci 3:615–623. https://doi.org/10.5194/nhess-3-615-2003

Spence R, Foulser-Piggott R (2014) The international macroseismic scale – extending EMS-98 for global application, Second European Conference on Earthquake Engineering and Seismology, Istanbul, Turkey

Stamps DS, Calais E, Saria E, Hartnady C, Nocquet JM, Ebinger CJ, Fernandes RM (2008) A kinematic model for the East African Rift. Geophys Res Lett 35(5):L05304

Supino M, Festa G, Zollo A (2019) A probabilistic method for the estimation of earthquake source parameters from spectral inversion: application to the 2016–2017 Central Italy seismic sequence. Geophys J Int 218(2):988–1007

Tedesco D, Badiali L, Boschi E, Papale P, Tassi F, Vaselli O, Kasereka C, Durieux J, DeNatale G, Amato A, Cattaneo M (2007a) Cooperation on Congo volcanic and environmental risks. Eos, Trans Ame Geophy Un 88(16):177–181

Tedesco D, Vaselli O, Papale P, Carn SA, Voltaggio M, Sawyer GM, Durieux J, Kasereka M, Tassi F (2007b) January 2002 volcano-tectonic eruption of Nyiragongo volcano, Democratic Republic of Congo. J Geophys Res: Solid Earth 112(B9).

Tertulliani A, Graziani L (2022) A critical overview of the January–February 1703 seismic sequence in central Italy. Bull Geophys Oceanoph 63:541–554. https://doi.org/10.4430/bgo00396

Tertulliani A, Arcoraci L, Berardi M, Bernardini F, Brizuela B, Castellano C, Ercolani E, Graziani L, Maramai A, Rossi A, Sbarra M (2012) The Emilia 2012 sequence: a macroseismic survey. Ann Geophys

Tertulliani A, Cecić I, Meures R, Sović I, Kaiser D, Grünthal G, Pazdirkova J, Sira C, Guterch B, Kysel R, Camelbeeck T, Lecocq T, Szanyi G (2018) The 6 May 1976 Friuli earthquake: re-evaluation and unifcation of transnational macroseismic data. Boll Geophys Teor App 59:417–444. https://doi.org/10.4430/bgta0234

Trendafiloski G, Wyss M, Rosset P (2011) Loss estimation module in the second generation software QLARM. In: Spence R, So E, Scawthorn C. (eds) Human Casualties in Earthquakes. Adv Nat Technol Hazards Res 29:95–106. https://doi.org/10.1007/978-90-481-9455-1_7

Trevlopoulos K, Gehl P, Negulescu C, Crowley H, Danciu L (2023) Testing the 2020 European Seismic Hazard and Risk Models using data from the 2019 Le Teil (France) earthquake. EGUsphere 2023:1–21

Triantafyllou I, Koukouvelas I, Papadopoulos GA, Lekkas E (2022) A reappraisal of the destructive earthquake (Mw5.9) of 15 July 1909 in Western Greece. Geosciences 12:374. https://doi.org/10.3390/geosciences12100374

Tringali G, Bella D, Livio F, Ferrario MF, Groppelli G, Blumetti AM, Michetti AM (2023) Fault rupture and aseismic creep accompanying the December 26, 2018, mw 4.9 Fleri earthquake (Mt. Etna, Italy): factors affecting the surface faulting in a volcano-tectonic environment. Quat Int 651:25–41

United States Geological Suvurvey (USGS) Earthquake Information, http://earthquake.usgs.gov/earthquakes/eventpage/us10002zzr

Vassallo M, Silvestri F, Pompa PP, Pietrosante A, Milana G, Gargiulo F, d'Onofrio A, Di Fiore V, Cosentino G, Coltella M, Cavuoto G (2021) Seismic microzonation in a complex volcano-tectonic setting: the case of northern and western Ischia Island (southern Italy). Ita J Geosc 140(3):382–408

Wald DJ, Quitoriano V, Heaton TH, Kanamori H, Scrivner CW, Worden CB (1999) Trinet ShakeMaps': rapid generation of instrumental ground motion and intensity maps for earthquakes in southern California. Earthq Spectra 15:537–556

Wang Z (2011) Seismic hazard assessment: issues and alternatives. Pure Appl Geophys 168:11–25

Wauthier C, Smets B, Keir D, Congo DR (2015) Geochem Geophys Geosyst 16: 4280–4291. https://doi.org/10.1002/2015GC006110

Weixiao X, Weisong Y, Dehu Y (2021) A real-time prediction model for macroseismic intensity in. China J Seismol 25:235–253

Wood HO, Neumann F (1931) Modified mercalli intensity scale of 1931. Bull Seismol Soc Am 21:277–283

Worden CB, Gerstenberger MC, Rhoades DA, Wald DJ (2012) Probabilistic relationships between ground-motion parameters and modified mercalli intensity in California. Bull Seismol Soc Am 102(1):204–221

Wu YM, Mittal H, Huang TC, Yang BM, Jan JC, Chen SK (2019) Performance of a low-cost earthquake early warning system (P-Alert) and shake map production during the 2018 M w 6.4 Hualien, Taiwan, earthquake. Seismol Res Lett 90(1):19–29

Xie J (2019) Strong-motion directionality and evidence of rupture Directivity effects during the Chi-Chi M w 7.6 earthquake. Bull Seismol Soc Am 109(6):2367–2383

Xie JJ, Wen ZP, Gao MT, Hu YX, He SL (2010) Characteristics of near-fault vertical and horizontal ground motion from the 2008 Wenchuan earthquake. China J Geophys 53(4):555–565

Yang Z, Chen WP (2010) Earthquakes along the East African Rift System: a multiscale, system-wide perspective. J Geophys Res Solid Earth 115:B12

Yang BM, Huang TC, Wu YM (2018) ShakingAlarm: a nontraditional regional earthquake early warning system based on time-dependent anisotropic peak groundmotion attenuation relationships. Bull Seismol Soc Am 108(3A):1219–1230

Yang BM, Mittal H, Wu YM (2021) Real-time production of PGA, PGV, intensity, and Sa ShakeMaps using dense MEMS-based sensors in Taiwan. Sens 21(3):943

Zanini MA, Hofer L, Faleschini F (2019) Reversible ground motion-to-intensity conversion equations based on the EMS-98 scale. Eng Struct 180:310–320

Authors and Affiliations

Francois Hategekimana[1,2] · Young-Seog Kim[1] · Himanshu Mittal[3] · Fils Vainqueur Byiringiro[2] · Mohammed S. M. Adam[1] · Digne Edmond Rwabuhungu Rwatangabo[2] · Sambit Prasanajit Naik[1,4]

✉ Sambit Prasanajit Naik
sambitnaik@gmail.com

1 Major of Environmental Geosciences, GSGR, Pukyong National University, Busan 48513, Republic of Korea

2 Department of Geology, College of Science and Technology, University of Rwanda, Kigali 3900, Republic of Rwanda

3 National Center for Seismology, Ministry of Earth Sciences, Govt. of India, New Delhi 110003, India

4 Active Fault and Earthquake Hazard Mitigation Research Institute, Pukyong National University, Busan 48513, Republic of Korea